

Brief Reports

Brief Reports are short papers which report on completed research which, while meeting the usual Physical Review standards of scientific quality, does not warrant a regular article. (Addenda to papers previously published in the Physical Review by the same authors are included in Brief Reports.) A Brief Report may be no longer than 3½ printed pages and must be accompanied by an abstract. The same publication schedule as for regular articles is followed, and page proofs are sent to authors.

Application of tridiagonalization to the many-body problem

J. D. Mancini and D. C. Mattis

Department of Physics, University of Utah, Salt Lake City, Utah 84112

(Received 11 August 1983)

The problem of a single magnetic, Wolff-model impurity in an otherwise ideal metallic host is investigated using the nonperturbative Lanczos method. Convergence is very rapid. The many-body ground-state energy is investigated and comparisons are made with Tomonaga operator theory and other weak-coupling schemes. We believe that this is the first application of tridiagonalization to the many-body problem.

I. INTRODUCTION

In this paper we approach the solution of a problem first posed over twenty years ago by Wolff.¹ A single impurity atom in a nonmagnetic host metal is considered, with no restriction placed on the number of electrons in the host conduction band. Wolff's original formulation was to treat the problem using the Hartree-Fock approximation and scattering theory while drawing upon the results of Koster and Slater² and also those of Friedel.³ The present study is a continuation of work initiated by one of us.⁴ The aim is to apply the nonperturbative Lanczos method proposed by Haydock, Heine, and Kelly⁵ to the Wolff model. To the best of our knowledge this work is the first application of tridiagonalization to the many-body problem, although a number of interesting many-body problems could be studied in this way.⁴ In the case of the Wolff model the impurity state interacts with some appropriate linear combination of conduction-band orbitals. This linear combination is then represented as the nearest-neighbor point to the impurity (chosen to be at the origin) on a semi-infinite linear lattice, which, in turn, interacts with some different linear combination, and so forth. Tridiagonalization is the mechanism by which this isomorphic mapping is accomplished; it is, in principle, an exact method.

II. WOLFF MODEL

The impurity is chosen to lie at the origin of the lattice. The only interaction of interest is the two-body Coulomb repulsion which is taken to be nonzero on the impurity, ignoring the Coulomb interaction between electrons in the conduction band of the host. All one-body interactions are absorbed by H_0 , which is diagonal,

$$H = H_0 + H' , \quad (1)$$

with

$$H_0 = \sum_k \epsilon_k n_k + W_0 , \quad (2)$$

where W_0 is chosen such that H_0 acting on the Fermi sea vanishes, $H_0|F\rangle = 0$, and

$$H' = \frac{1}{4} U \quad , \quad (3)$$

where U is the Coulomb repulsion at the impurity site and

$$\Omega = \Omega^\dagger = (2n_{0\uparrow} - 1)(2n_{0\downarrow} - 1) , \quad (4)$$

with

$$n_{0\sigma} = \frac{1}{N} \sum_{k,k'} c_{k\sigma}^\dagger c_{k'\sigma} . \quad (5)$$

We shall focus our attention on the half-filled symmetric band for which

$$\langle F | n_{0\sigma} | F \rangle = \frac{1}{2}, \quad \Omega^2 = 1, \quad \langle F | \Omega^{2p+1} | F \rangle = 0, \quad (6)$$

$$p = 0, 1, 2, \dots$$

These identities play a crucial role in the simplifying of various matrix elements generated by the tridiagonalization recursion method which we briefly outline in Sec. III.

III. METHOD

Prior to this study the use of the tridiagonalization had been primarily restricted to density-of-states calculations in regions where Bloch's theorem is no longer valid, i.e., surfaces, dislocations, amorphous materials, and so forth.⁶ The main thrust of this paper is an evaluation of the many-body ground state $E_0(U)$. The crucial first step in the method lies in the choice of an initial state $|\phi_0\rangle$, chosen either for its symmetry classification or for its computational simplicity. Once the initial state is chosen an orthogonal set of states $\{|\phi_n\rangle\}$ is generated according to the following schema:

$$H|\phi_i\rangle = m_{i,i-1}|\phi_{i-1}\rangle + m_{i,i}|\phi_i\rangle + m_{i,i+1}|\phi_{i+1}\rangle . \quad (7)$$

Also being generated is the tridiagonal Hermitian matrix \tilde{M} , the elements of which m_{ij} are nonzero only for $i=j$ or

$i = j \pm 1$. As previously noted⁴ a variational upper bound on the ground-state energy E_0 may be obtained by the direct diagonalization of any submatrix of \tilde{M} . In this work we have calculated explicitly the matrix elements of \tilde{M} up to dimensions 4×4 . As a consequence, we also obtain expressions for $E_0^{(2)}(U)$, $E_0^{(3)}(U)$, and $E_0^{(4)}(U)$, where the superscript refers to the size of the submatrix of \tilde{M} . Then by plotting these points as a function of $1/n$, where $n = 1, 2, 3, 4$ is the size of the submatrix, we extrapolate to $n \rightarrow \infty$ ($1/n \rightarrow 0$) which is just the y intercept. Hence, by reading off the values of the y intercept for each value of U , we are able to obtain accurate estimates for the ground-state energy, denoted by $E_0^{(\infty)}$. We then compare our results for $E_0^{(\infty)}$ with those of second-order perturbation theory and strong-coupling theory, both of which are known exactly.

$$\langle F | \Omega H_0 \Omega | F \rangle = \langle F | \Omega [H_0, \Omega] | F \rangle = \frac{2}{N} \sum_{l,2} \sum_{\substack{\sigma, \sigma' \\ \sigma \neq \sigma'}} \langle F | \Omega (2n_{0\sigma} - 1) c_{2\sigma}^\dagger c_{1\sigma'} | F \rangle (\epsilon_2 - \epsilon_1) \quad (9)$$

it follows that matrix elements of the form $\langle F | \Omega H_0^l \Omega | F \rangle$, $l = 1, 2, 3, \dots$, may be evaluated as a sequence of commutators. Once this is accomplished one may evaluate the integrals over the energies using (8). Table II gives the algebraic expressions for the matrix elements m_{ij} and their numerical values.

Once the m_{ij} have been calculated, one obtains ground-state energies $E_0^{(2)}(U)$, $E_0^{(3)}(U)$, and $E_0^{(4)}(U)$, shown in Fig. 1(a). In order to obtain an expression for $E_0^{(\infty)}$ one plots $E_0^{(n)}$ for a fixed value of U , as a function of $1/n$. In Fig. 1(b) we have chosen the values $U = 1, 2$, and 3 for illustration. The y intercept of these curves, $n = \infty$ ($1/n = 0$) corresponding to $E_0^{(\infty)}(U)$, is extrapolated to fit a curve, comprised of the four points $E_0^{(1)}(U) = 0$, $E_0^{(2)}(U)$, $E_0^{(3)}(U)$, and $E_0^{(4)}(U)$, by standard methods. The error in the point $E_0^{(\infty)}(U = 0.25)$ is 1% and for $E_0^{(\infty)}(U = 5)$ is 0.238%. The coefficient of U^2 in second-order perturbation theory is -0.0697 . In the weak-coupling regime our result for $E_0^{(\infty)}(U)$ follows a parabola with coefficient -0.0698 . For large coupling, $E_0^{(\infty)}(U)$ approaches the straight line $E_0^{(\infty)}(U) = -0.25U + 0.214$.

As is usually the case in physics, the region of intermediate coupling is also the region of most interest and frequently the most difficult to solve. Figure 1(a) affords us the luxury of looking graphically at this situation. We see that for values of U less than 1, $E_0^{(\infty)}$ follows rather closely the

TABLE I. Matrix elements in the explicit calculation of the m_{ij} .

$$\begin{aligned} \langle F | \Omega H_0 \Omega | F \rangle &= 1 \\ \langle F | \Omega H_0^2 \Omega | F \rangle &= 1.08333 \\ \langle F | \Omega H_0^3 \Omega | F \rangle &= 1.25 \\ \langle F | \Omega H_0^4 \Omega | F \rangle &= 1.51875 \\ \langle F | \Omega H_0^5 \Omega | F \rangle &= 1.9270833 \\ \langle F | \Omega H_0 \Omega H_0 \Omega | F \rangle &= 0 \\ \langle F | \Omega H_0 \Omega H_0^2 \Omega | F \rangle &= 0 \\ \langle F | \Omega H_0 \Omega H_0 \Omega H_0 \Omega | F \rangle &= 3.7045477 \end{aligned}$$

IV. RESULTS AND CONCLUSIONS

In this work we have chosen a flat density-of-states symmetric about the Fermi level:

$$\rho(\epsilon) = \begin{cases} 1, & -\frac{1}{2} \leq \epsilon \leq \frac{1}{2} \\ 0, & \text{otherwise} \end{cases} \quad (8)$$

We also choose our initial state $|\phi_0\rangle$ to be the Fermi sea $|F\rangle$ (thus $|\phi_1\rangle = -\Omega|F\rangle$), since it is well known⁷ that the ground state must be a singlet which reduces to $|F\rangle$ when $U = 0$. Repeated application of H upon $|\phi_0\rangle$ according to Eq. (7) gives the desired results. Table I lists the type of matrix elements one encounters in the explicit calculation of the m_{ij} . With the matrix identity

TABLE II. Algebraic expressions for the matrix elements m_{ij} and their numerical values.

$$\begin{aligned} m_{00} &= 0 \\ m_{01} &= -\frac{U}{4} = m_{10} \\ m_{11} &= \langle F | \Omega H_0 \Omega | F \rangle = 1 \\ m_{12} &= -[\langle F | \Omega (H_0 - m_{11})^2 \Omega | F \rangle]^{\frac{1}{2}} = -\frac{1}{\sqrt{12}} = m_{21} \\ m_{22} &= \frac{1}{m_{12}^2} \langle F | \Omega (H_0^3 - 2H_0^2 m_{11} + H_0 m_{11}^2) \Omega | F \rangle = 1 \\ m_{23} &= -\left\{ \frac{1}{m_{12}^2} [\langle F | \Omega H_0^4 \Omega | F \rangle - 2(m_{11} + m_{22}) \langle F | \Omega H_0^3 \Omega | F \rangle \right. \\ &\quad + (m_{11}^2 + m_{22}^2 + 4m_{11}m_{22} + \frac{U^2}{16}) \langle F | \Omega H_0^2 \Omega | F \rangle \\ &\quad - 2(m_{11}^2 m_{22} + m_{11} m_{22}^2 + m_{11} \frac{U^2}{16}) + m_{11}^2 \frac{U^2}{16} + m_{11}^2 m_{22}^2] \\ &\quad + 2 \langle F | \Omega H_0^2 \Omega | F \rangle - 2m_{11} \langle F | \Omega H_0 \Omega | F \rangle + m_{21}^2 \Big\}^{\frac{1}{2}} \\ &= -[0.2249976 + \frac{U^2}{16}]^{\frac{1}{2}} = m_{32} \\ m_{33} &= \frac{1}{m_{23}^2} \left\{ \frac{1}{m_{21}^2} [\langle F | \Omega H_0^5 \Omega | F \rangle - 2(m_{11} + m_{22}) \langle F | \Omega H_0^4 \Omega | F \rangle \right. \\ &\quad + (m_{11}^2 + m_{22}^2 + 4m_{11}m_{22} + \frac{U^2}{8}) \langle F | \Omega H_0^3 \Omega | F \rangle \\ &\quad - 2(m_{11}^2 m_{22} + m_{11} m_{22}^2 - m_{11} \frac{U^2}{8} - m_{22} \frac{U^2}{16}) \langle F | \Omega H_0^2 \Omega | F \rangle \\ &\quad + (m_{11}^2 m_{22}^2 + m_{11} m_{22} \frac{U^2}{4} + m_{11}^2 \frac{U^2}{8}) \langle F | \Omega H_0 \Omega | F \rangle \\ &\quad + \frac{U^2}{16} \langle F | \Omega H_0 \Omega H_0 \Omega H_0 \Omega | F \rangle - m_{11}^2 m_{22}^2 \frac{U^2}{16} \Big\} \\ &\quad + 2 \langle F | \Omega H_0^3 \Omega | F \rangle - 2(m_{11} + m_{22}) \langle F | \Omega H_0^2 \Omega | F \rangle \\ &\quad + 2(m_{11} m_{22} + m_{21}^2 + \frac{U^2}{16}) \langle F | \Omega H_0 \Omega | F \rangle - m_{11}^2 \frac{U^2}{16} \Big\} \\ &= \frac{0.475 + 2.7784108U^2}{0.2249976 + 0.0625U^2} \end{aligned}$$

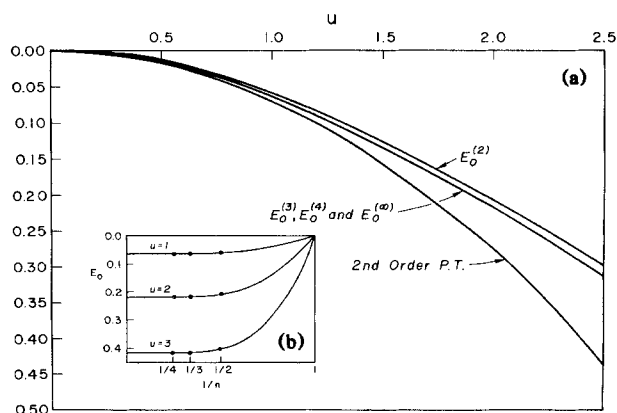


FIG. 1. (a) Results from tridiagonalization (read from top to bottom) for $E_0^{(2)}(U)$, $E_0^{(3)}(U)$, $E_0^{(4)}(U)$, and $E_0^{(\infty)}(U)$, and for second-order perturbation theory (on this scale, $E_0^{(3)} \geq E_0^{(4)} \geq E_0^{(\infty)}$ are indistinguishable). (b) (insert) Illustrating rapid convergence: E_0^n is plotted as a function of $1/n$, where n is the dimension of the matrix \tilde{M} . The values of $U=1, 2$, and 3 are chosen for illustration.

parabola of second-order perturbation theory. It is for U between 1 and 2 that $E_0^{(\infty)}$ appears to be making its most drastic change, and begins to resemble a straight line. We interpret this to mean that in the range $U=1$ to $U=2$ a

transition between the weak- and the strong-coupling regimes is taking place.

An advantage of the tridiagonalization scheme is that it permits us to examine E_0 as a function of the complex variable U . The simplest calculation for \tilde{M} of dimension 2×2 yields branch points at $U = \pm 2i$, thus limiting small- U expansions to $|U| < 2$ (see Ref. 4). Further calculation on the 3×3 matrix yields four branch points, those closest to the origin being at $U = \pm(1.718)i$. We have not carried the analysis out to 4×4 , but note that m_{23} vanishes at $U = \pm(0.89)i$, and m_{33} at $\pm(0.413)i$.

Now the weak-coupling schemes *all* break down at a critical U (see Ref. 8). For example, the magnetic susceptibility in the Tomonaga-operator scheme⁹ diverges at $U=1$. We can now appreciate that this is due to the failure of power-series expansions beyond their radius of convergence, which the present analysis has served to locate. This may be one of the principal applications of tridiagonalization in the many-body problem—the location of *critical parameters*, whether on the real axis where they signify real phase transitions, or in the complex plane, whence they might be excised in the well-known manner of Padé approximations.¹⁰

ACKNOWLEDGMENT

This research has been supported by the National Science Foundation under Grant No. DMR-81-06223.

¹P. A. Wolff, Phys. Rev. **124**, 1030 (1961).

²G. F. Koster and J. C. Slater, Phys. Rev. **96**, 1208 (1954).

³J. Friedel, Nuovo Cimento Suppl. **7**, 287 (1958).

⁴D. C. Mattis, in *Physics in One Dimension*, edited by J. Bernasconi and T. Schneider, Springer Series in Solid-State Sciences, Vol. 23 (Springer, New York, 1981).

⁵R. Haydock, V. Heine and M. J. Kelly, J. Phys. C **5**, 2854 (1972); **8**, 2591 (1975).

⁶R. Haydock, J. Phys. A **10**, 461 (1977); in *Solid State Physics: Advances in Research and Applications*, Vol. 35, edited by F. Seitz and

D. Turnbull (Academic, New York, 1980), p. 215.

⁷D. C. Mattis, Phys. Rev. Lett. **19**, 1478 (1967).

⁸H. C. Fogedby, J. Phys. C **10**, 2869 (1977).

⁹D. C. Mattis, Ann. Phys. (N.Y.) **89**, 45 (1975). Note that, in comparing with the present work, one divides the U in the earlier by two and sets the momentum cutoff $q_0 = \pi$ (so that the band edges are at $\omega = \pm \frac{1}{2}$).

¹⁰*The Padé Approximant in Theoretical Physics*, edited by G. A. Baker, Jr. and J. L. Gammel (Academic, New York, 1970).